American Journal of Physics and Applications
2022; 10(5): 62-71
http://www.sciencepublishinggroup.com/j/ajpa
doi: 10.11648/j.ajpa.20221005.11
ISSN: 2330-4286 (Print); ISSN: 2330-4308 (Online)

Investigation of Mixed Transition Effect in MnO_2 AND V_2O_5 Doped Ternary Borate Glass System

Sangamesh Jakhati[1], Nagaraja Nadavalumane[1, *], Ashwajeet Jalandhar Rao Sonkamble[2]

[1]Department of Physics (VTU-Research Centre), Rao Bahadur Y Mahabaleswarappa Engineering College, Ballari, India
[2]Department of Physics, Davangere University, Davanagere, India

Email address:

nagphysics@gmail.com (Nagaraja Nadavalumane)
[*]Corresponding author

To cite this article:

Sangamesh Jakhati, Nagaraja Nadavalumane, Ashwajeet Jalandhar Rao Sonkamble. Investigation of Mixed Transition Effect in MnO_2 AND V_2O_5 Doped Ternary Borate Glass System. *American Journal of Physics and Applications*. Vol. 10, No. 5, 2022, pp. 62-71.
doi: 10.11648/j.ajpa.20221005.11

Received: October 1, 2022; **Accepted**: October 17, 2022; **Published**: October 29, 2022

Abstract: A novel ternary borate glass system was synthesized by utilizing standard melt quench approach. All of the samples went through an annealing process for 6 hours to remove retained thermal strains present in glass structure. XRD test revealed that the samples were indeed glassy. Density was determined at room temperature; oxygen packing density (OPD) and molar volumes were calculated. Both density and OPD changes followed recognizable patterns that complemented the Mixed Transition Effect (MTE). The electrical resistivity was measured by Keithley two probe instrument in range of temperatures 308-523K and conductivity was estimated. These glasses are unique among single TMI doped glasses systems in that they have exceptionally high conductivities in 10^{-5} to 10^{-3} $(\Omega m)^{-1}$ range, while still maintaining low activation energies. The conductivity data was analyzed through Motts small polaron hopping (SPH) model at higher temperature region $T > \theta_D/2$ and remaining data was analyzed by employing the VRH models by Mott's, Mott-Greave's at lower temperature region $T < \theta_D/2$. Respective polaron related parameters such as small polaron radii, the average distance between transition metal ions, TMI density, mobility etc. were estimated. The very first time, by using a MnO_2-V_2O_5 dopant ternary borate glasses have been synthesized. Studies on high-and low temperature DC conductivity investigations have revealed the presence of a mixed transition effect (MTE).

Keywords: Borate Glasses, TMI, Mott's SPH Model, Mixed Transition Effect (MTE), DC Conductivity

1. Introduction

Glasses are ever more fascinated due to their advantages over crystalline materials owing to their easy formability over a wide range of composition, nonappearance of grain boundaries, ease of production into complex shapes. The amorphous oxide glasses have protruding role to play in the field of electronics, computer memories, space research, nuclear shielding and medical field [1-4]. Since from last four to five decades electrical conductivity in oxide glass systems [5-7] such as borate, silicate, phosphate, vanadate, and tellurite glasses doped with transition metal ions for example Cu, Al, Zn, Fe, V, Co etc has been a great interest of study. Amongst all the various types of oxide glasses, the borate is a very important and well-known glass former owing to its low melting point, high transparency and high thermal stabilities. The structure of amorphous B_2O_3 is a planar BO_3 triangles connected through BO-B connections. Addition of network modifiers to pure B_2O_3 glass might produce either in the change of triangular BO_3 units into BO_4 tetrahedral or non-bridging oxygen atoms (NBOs). The network modifiers such as transition metal ions when added in appropriate amounts to amorphous B_2O_3 glass network, brings about semiconducting nature in glasses. Borate glasses doped with appropriate transition metals ion resulted in the application of rechargeable batteries, owing to the multivalent states of the transition metals ions. Amongst various transition metal oxides, the multivalent V_2O_5 is an important semiconductor and at many instances in glass matrix it plays the role of both as a glass former and also a network modifier [22–24].

Another interesting TM oxide is Manganese dioxide, since it is a fairly common component in the field of batteries, in which contexts it has been employed as the positive electrode [25]. MnO_2 is a strong oxidant, relatively inexpensive, and abundant, thus making it a top candidate for use as a positive electrode in lithium cells. Manganese dioxide is not only an essential integral component in lithium based rechargeable batteries [26] but also used in cobalt and zinc based rechargeable batteries as well, some groups of researchers have also confirmed that manganese-based batteries is being developed as an alternative to both cobalt and lithium rechargeable batteries owing to their toxicity and expensive maintenance [27]. Many investigations like NMR, EPR, FTIR & Raman studies on MnO_2 doped borate glasses are available in the literature [28–31]. There are hardly few investigations on electrical conductivity and other polaron related properties of MnO_2 and V_2O_5 doped borate glasses.

Hence in our present study, we have prepared novel series of ternary borate glass system in the following composition range $\{B_2O_3\}_{0.5}$ - $\{V_2O_5\}_{(0.5-x)}$ - $(2MnO_2 2)_x$ coded as BVM glass with $x = 0.05, 0.1, 0.15, 0.2, 0.25, 0.3$, for the first time deliberating the investigations on the mechanism of DC conductivity and presenting it in this research paper.

2. Experimental Method

On immediate availability basis, all AR grade chemical ingredients with ≥99% purity were purchased from different international chemical manufacturers such as boron oxide (B_2O_3) from otto, both vanadium oxide (V_2O_5) and Manganese (IV) oxide from Sigma-Aldrich. In accordance to the calculated weight proportion for each glass sample, individual chemicals were mixed in appropriate amount and transferred into an agate mortar. The mixtures manually grinded to obtain a fine powder under molecular dimensions. The mixture, then shifted into silicon crucibles procured from infusil brand scientific company. The crucible is placed into a high temperature electrical muffle furnace and was heated to a very high temperature of the order of 1253 K and left over for 2 hours. When the melted homogenized colorless mixture of the liquid was formed, then the liquid quickly poured into a fine stainless-steel mould kept at room temperature by suddenly closing another same stainless-steel plate on to it. The random pieces of the glasses were collected. Following the same method, all the other glasses compositions with chosen mole fractions of x = 0.05, 0.1, 15, 0.2, 0.25, 0.3, were synthesized. The glasses were annealed at 523 K for about six hours to remove if any thermal strains present in the glass metrics. The samples were made fine dimensions by polishing using fine sand paper to a varying thickness and area.

2.1. XRD

Studies using X-ray diffraction were carried out on each and every one of the synthesized glasses. With XRD instrument specifications; Malvern Panalytical X-ray diffractometer X'PERT^3 powder instrument operated at 40 kV and current of 30mA with $Cu - K\alpha - 1$ wavelength- 1.54060Å and $Cu - K\beta$ wavelength- 1.39225Å with the ratio $K\alpha - 1$ =0.5 at room temperature between 2θ ranging from 5 to 80 degree.

2.2. Density

Density (ρ), examinations on the glasses were performed at room temperature utilizing the Archimedes principle and a citizen made single pan digital balance accurate to 0.1 mg with toluene ($\rho_{Toluene}$ = 0.8669 g/CC) as the immersion liquid.

2.3. Measurement of DC Conductivity

The glass samples appropriately cut into fine dimensions were measured thickness ranging from 1.45 - 3.08 mm and areas 21 mm^2 to 71 mm^2. The dc electrical conductivity measurement was carried by applying conductive silver paste on either side of the large surfaces then transferred them in a two probe Keithley made instrument. The current flowing through glasses were enumerated by digital picometer with accuracy of 0.0001 pA by applying constant voltage across the glasses over a wide temperature, ranging from 303K to 523K. Chromel-alumel thermocouples were used to gauge sample temperatures with ±1K precision. A determination of conductivity was made using $\sigma = 1/\text{resistiity}$, here resistivity calculated by $Resistivity = R.A/r$ Here, R represents resistance, A represents cross sectional area, and r represents the glass samples' thickness. According to the relation, $\Delta\sigma = [\Delta Resitivity/\sigma^2]$ here error in Resistivity $= [(\Delta V/V) - (\Delta I/I)]$, approximated the error on conductivity, taking into consideration the inaccuracies on the observed voltages and currents. An inaccuracy of 5% is determined to encompass the anticipated conductivity errors.

3. Results and Discussions

3.1. X-ray Diffraction Studies

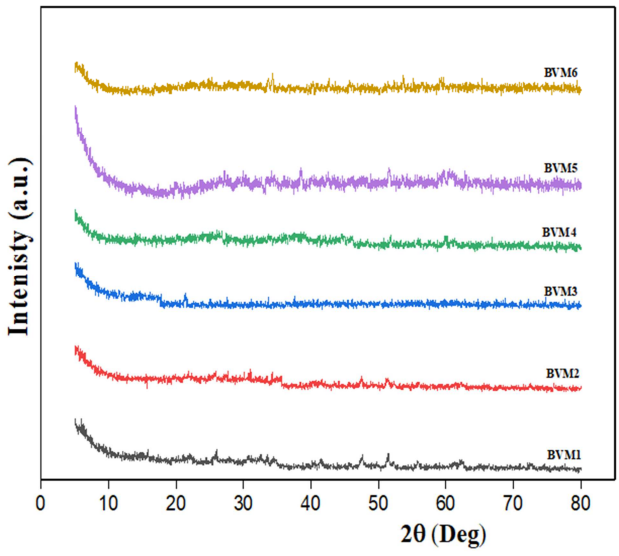

Figure 1. *X-ray diffraction spectra of BVM glasses.*

Spectra obtained by X-ray diffraction analysis of annealed

BVM glasses did not show any sharp peaks in the depicted figure 1, hence it was concluded that all the samples are non-crystalline in nature [32–34].

3.2. Density and Molar Volume

The density (ρ), was determined using the formula, $\rho = \left[\frac{W}{W-W_L}\right].\rho_L$, here W represents the glass's weight in air, W_L represents the glass's weight in toluene, ρ_L represents toluene's density. The molar volume V_m for BVM glasses was calculated using $M_V = \left[\frac{m}{D}\right]$, here m is glass's Molecular weight. The determined density at room temperature (ρ) with calculated molar volume (M_V) of BVM glasses were found to be in the range of 1.200 g/cm^3 to 2.629 g/cm^3 and 47.07 cm^3/mol to 104.14 cm^3/mol respectively are enumerated in following Table 1. Following figure 2, shows the variations of density ρ, Vs Molar volume M_v and similar varying plot of molar volume with oxygen packing density against varying mole fraction of MnO_2 content is depicted in figure 3.

It is clear from both figure 2 and figure 3 that first density and OPD (oxygen packing density) decreased slightly at 0.10 mole fraction with increase of MnO_2 concentration, but then afterwards density and OPD increasing continuously [35] and attained highest value at 0.25 mole fraction of MnO_2 content in glass matrix, thus hinting in the increased compactness with more number of oxygen containing structures (from figure 2) in the glass network [36–38] from BVM1 to BVM5, then onwards for BVM6 glass network gets slightly relaxed due to sudden diminished oxygen packing and density at 0.30 mole fraction of MnO_2 content in the glass matrix. Hence, the 0.25 mole fraction of MnO_2 is the point of mixed transition effect. But, the molar volume M_v in figure 2 and figure 3 has behaved exactly in opposite manner to the variations of density and OPD, reaching minimum at 0.25 mole fraction of MnO_2 and hitting highest value at 0.1 mol fraction of MnO_2 concentration in the glass matrix [39–43]. The BVM glass matrix consist of Manganese (Mn) and Vanadium (V) transition metal ions (TMIs), thus the conductivity is due to both of these TMIs. The TMI density N of the corresponding TMI ions are computed by using the subsequent formula [44] and presented in table 1 $N = 2\left\{\left(\frac{\rho.W_t}{m}\right)N_A\right\}$, Here ρ signifies density, W_t signifies weight mole fraction, m is the molecular Wt. of the respective TMI with N_A being Avogadro number. Thus, concentration of manganese ions and vanadium ions are in the range of 0.536-5.581 cm^{-3} and 2.419-3.762 cm^{-3} respectively. The small polaron radii r_p[45] the average distance between transition metal ions which is denoted by R. [46] with oxygen packing density (OPD) individually all are computed and listed in table 1 [47].

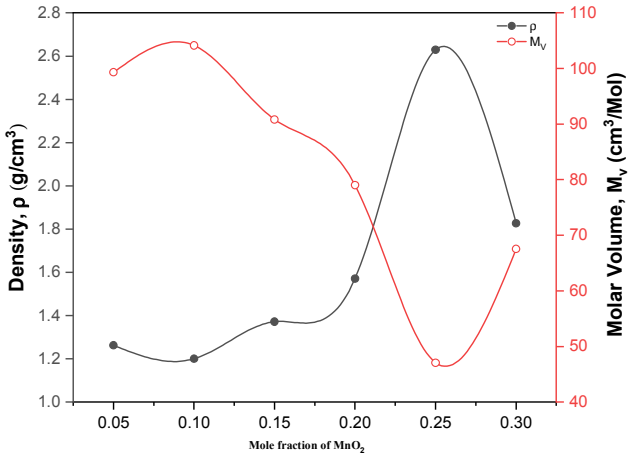

Figure 2. *Plot of Density and molar volume Vs Mole fraction of MnO_2*

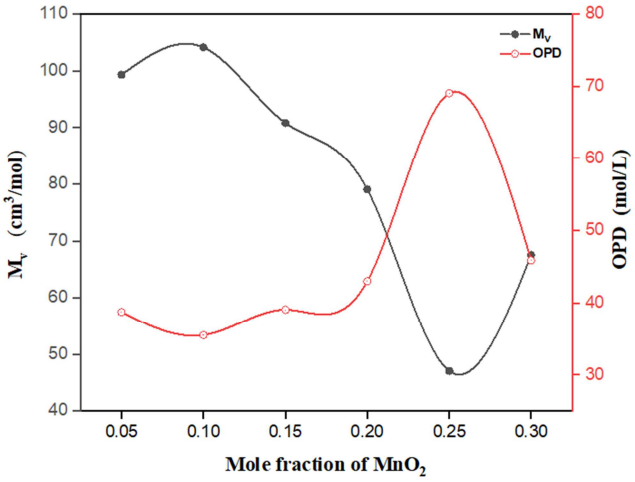

Figure 3. *Plot of Molar volume and Oxygen packing density Vs Mole fraction of MnO_2.*

Table 1. *Physical Properties of BVM glasses.*

Glass Sample	MnO_2 x	ρ g/cm^3	M_v cm^3/mol	OPD Mol/L	R nm	r_p nm	N-2MnO× 10^{21} cm^{-3}	N-V_2O_5× 10^{21} cm^{-3}	N×10^{21} (N-2MnO+ N-V_2O_5) cm^{-3}
BVM1	0.05	1.262	99.31	56.11	1.045	0.422	0.536	3.762	4.298
BVM2	0.1	1.200	104.14	35.53	0.844	0.340	1.019	3.179	4.197
BVM3	0.15	1.371	90.83	74.93	0.705	0.284	1.746	3.179	4.925
BVM4	0.2	1.571	79.04	37.55	0.612	0.247	2.667	3.121	5.789
BVM5	0.25	2.629	47.07	33.14	0.479	0.193	5.581	4.354	9.935
BVM6	0.3	1.827	67.53	39.48	0.509	0.205	4.653	2.419	7.072

3.3. DC Conductivity Studies

The measured DC conductivity of all BVM glasses with respect to temperature variations are fond to be in the range of $3.59 \times 10^{-5}(\Omega m)^{-1}$ to $2..14 \times 10^{-3}(\Omega m)^{-1}$ [48] the figure 4 shows plot of conductivity (σ) variation of all the BVM glasses with increase in temperature (T) the nature of the plots reveals that BVM glasses are semiconducting in

nature, for clarity single zoomed plot of BVM3 glass conductivity (σ) Vs Temperature (T) has been shown inside the figure 4 [10]. In figure 4, higher temperature region of the conductivity $T > \theta_D/2$,, here θ_D is the Debye temperature and T represents the temperature where conductivity starts to vary from Mott's SPH model, the plots exhibit linear variation of conductivity and this zone of the graph was examined using Mott's small polaron hopping model. [11, 21, 46, 49] the graph of ln(σT) Vs (1/T) were plotted for current BVM glasses and exhibited in figure 5. In high temperature region, the activation energy W was determined via linear least square fits to the respective BVM glass conductivity data, W values that ranged between 0.280-0.558 eV and same are having close agreement in literature [39, 41].

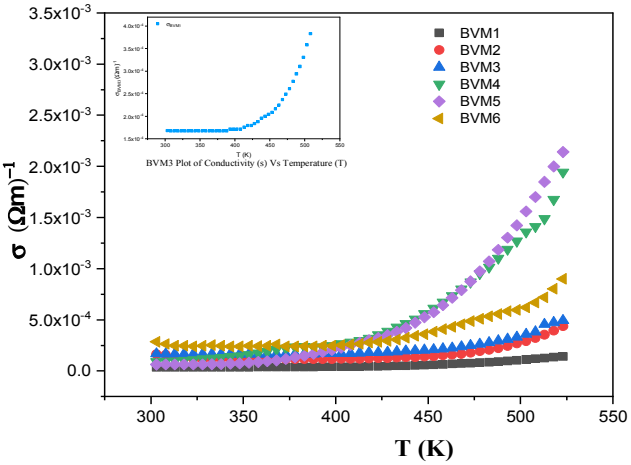

Figure 4. *Plot of conductivity Vs Temperature of BVM glasses.*

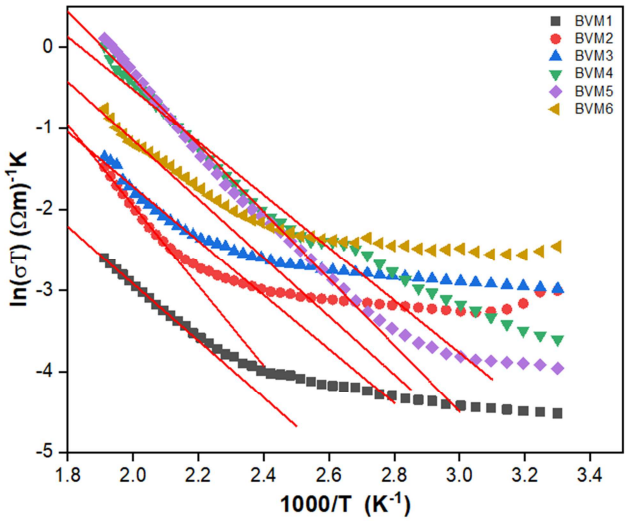

Figure 5. *Plot of ln (σT) Vs (1/T). Solid lines are LS fits to BVM glasses curves.*

In figure 6, both activation energy (W) and conductivity (σ) data are displayed against alterations in the mole fraction of MnO_2 content. It is evident from figure 6 that conductivity keeps rising until 0.25 mole fraction of MnO_2 concentration, and this highest value of conductivity may be correlated with the high temperature zone of Figure 4 for the same BVM5 glass sample. Again, this is seen in Figure 6, where the conductivity value drops down precipitously after the 0.25 mole fraction of MnO_2 is added. In contrast to conductivity, low values of activation energy, W acted almost oppositely. The same sort of behavior in activation energy and conductivities is reported for such a mixed TM ion doped borate glasses systems [11, 41, 47, 50].

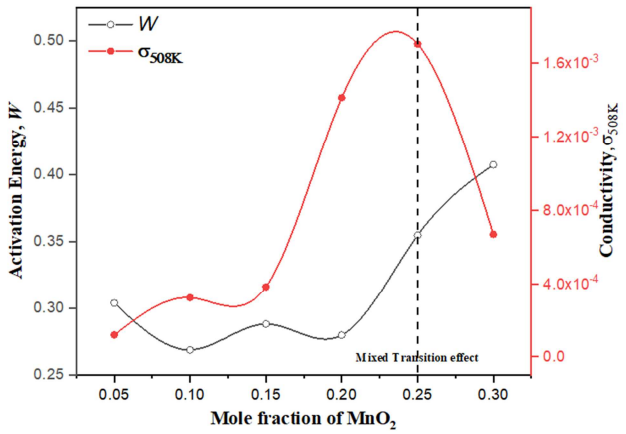

Figure 6. *Mole fraction variation of Activation energy and conductivity at 508K.*

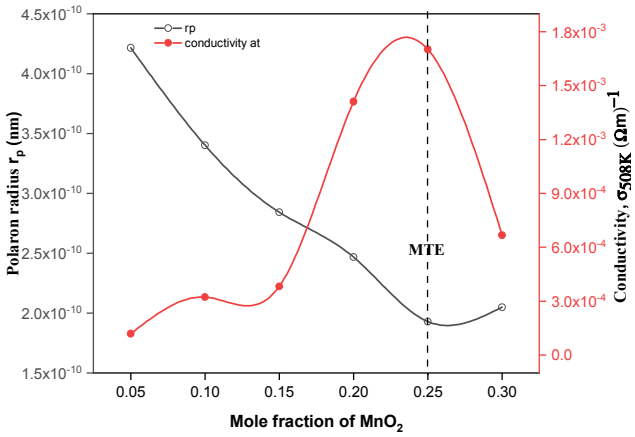

Figure 7. *Mole fraction variation of Polaron radius and conductivity at 508K.*

The exceptionally high conductivities and low activation energies of BVM glasses sets them apart from all other single TMI doped glasses systems documented in the literature due to the role of cation's partial charge in glass formation oxides [51] and also possible contribution owing to V_2O_5, which provides glass-forming transition metal ions [52, 53] playing double role that is first they act as ionic cites for Polarons hopping conduction and second, they also take part in the conduction mechanism by diffuse of V^{4+} and V^{5+} ions into the glass matrix because manganese is not a glass former [11, 54, 55].

It is well accepted that elements like vanadium, manganese, and other transition metal ions (TMI) can exist in several valency states [49]. It is plausible that the higher conductivity value at 0.25 mole fraction of MnO_2 content (from table 1) is related to higher charge carrier concentrations (N-2MnO+N-

V2O5) owing to vanadium and manganese ions (mixed transition effect) (V^{+4}, V^{+5}, and Mn^{+2} and Mn^{+3}) in comparison to the other compositions in our existing BVM glass systems, Notably, with change in composition; as manganese ion concentration increases, proportionately vanadium ion concentration decreases till both attains maximum value at 0.25 mole fraction and thus creating more number of TMIs available for hopping between two dissimilar ions Mn^{+2} to V^{+4}, Mn^{+3} to V^{+5} but conductivity declines sharply with increasing MnO_2 concentration, at the expense of V_2O_5, above the 0.25% threshold, demonstrating a mixed transition effect (MTE) [11]. The variations in conductivity has been shown to have an inversely related relationship to the polaron radius, denoted by r_p, as seen in Figure 7. DC conductivity studies in V_2O_5-MnO-TeO_2 glass system, revealed decrease in conductivity values with respect to increase in TeO_2 and MnO concentrations in glass matrix. In both systems, increasing disorder energy and declining conductivity were found [13, 50]. As conductivity diminishes, polaron radius, r_p and mean distance, R between transition metal ions grow. But in another P_2O_5-V_2O_5-Fe_2O_3 glass system the decrease in conductivity was followed by increase in r_p and R thus followed by increased configurational disorder in contrary to the decrease in conductivity [41]. In some other glass systems viz; Fe_2O_3-B_2O_3-V_2O_5 and B_2O_3-V_2O_5-MoO_3 it was observed that as the concentration of glass modifiers went up, the conductivity of these glass systems went up. This was followed by a negative correlation between changes in r_p and R and a decrease in the system's disorder energy at higher conductivity values [47, 41]. But again, it was also be noted in these Fe_2O_3-MgO-TeO_2, P_2O_5-V_2O_5-MnO and CoO_3-V_2O_5-B_2O_3, glass systems, while both r_p and R grow as conductivity goes up [11, 45, 56] it's important to remember that r_p decreases as conductivity goes up to very high values. With that discussed, Enhancement of conductivity depends not only on charge carrier concentrations, polaron radius but also on many other aspects, such as the redox ratio in the glass network, disorder energy, influence of the cations' partial charges on the glass-forming oxides, Anderson's localization [57–60].

3.4. Small Polaron Hopping Parameters

The W_H and W_D are the disorder and polaron hopping energies, respectively that can exist between the interstitial ionic sites in the glass matrix were likely to be dominated by the activation energy W at high temperatures, where nearest-neighbor thermally induced hopping is the dominant hopping mechanism. [61] For systems allowing for robust electron phonon interactions, Austin and Mott recommended [62],

$$W = W_H + W_D \quad T > \theta_D/2$$

$$\cong W_D \quad T < \theta_D/4$$

Here, $W_H = W_p/2 = \{e^2/4\varepsilon_p\}[r_p^{-1} - R^{-1}]$ is polaron hopping energy [46] and estimated to be in the range of 0.161 eV to 0.243 eV [47], because of the energy disparity between two hopping sites disordered energy W_D is produced and is found in range of 0.226 eV to 0.450 eV, W_p is the polaron binding energy which is ranging from 0.321 eV to 0.487 eV is similar to [11], the effective dielectric constant, denoted by ε_p, varying between 35.297 to 66.023 was found to behave exactly the same way to that of conductivity over the Debye temperature range θ_D . The small polaron radius $r_p = (1/2)(\pi/6N)^{1/3}$ [13, 63] and various estimated small polaron parameters are listed in the Table 2. Understanding of polaron bandwidth, J_{SPH} encompasses the knowledge of the overlap of wavefunction of adjacent sites for adiabatic and non-adiabatic regimes in Small polaron hopping model,

$$J_{SPH} > \left(\frac{2kTW_H}{\pi}\right)^{1/4} \cdot \left(\frac{h\nu_o}{\pi}\right)^{1/2} \text{ for adiabatic SPH}$$

$$J_{SPH} < \left(\frac{2kTW_H}{\pi}\right)^{1/4} \cdot \left(\frac{h\nu_o}{\pi}\right)^{1/2} \text{ for non-adiabatic SPH}$$

The polaron bandwidth J_{SPH} can also be calculated form the equation $J = J_o \exp(-2\alpha R)$ best matches with [64] here $J_o = W_H/4$ the calculated values are shown in table 3, further, the value $\alpha = 20nm^{-1}$ is in accordance with literature of TMI doped glasses [13, 65]. Its evident form the table 3 data of polaron bandwidth that J_{wh} satisfies the non-adiabatic SPH condition and also Holstein condition for small polaron hopping [66]. The small polaron coupling constant γ_P is important in knowing the electron-phonon interaction and is computed by relation $\gamma_P = 2W_H/h\nu_o$ and is presented in the table 3 from same data its clearly obvious that, the small polaron coupling constant γ_P value is stronger at 0.25 mole fraction of MnO_2 at which conductivity in table 2 is possessing higher value. Consequently, conductivity and the small polaron coupling constant demonstrate a clear direct link with one another in BVM glasses.

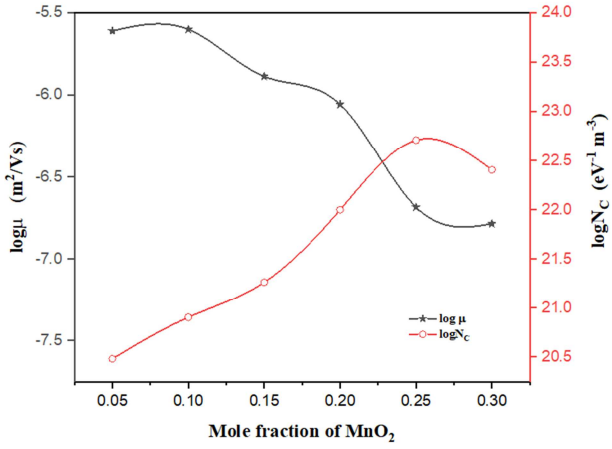

Figure 8. *Plot of $\log \mu$ and $\log N_C$ Vs Mole fraction of MnO_2 in BVM glasses.*

The carrier mobility μ in the adiabatic and non-adiabatic region is due to diffusion of electron by small polaron hopping [46, 62] the carrier mobility μ for present BVM glasses were calculated at temperature of 508 K and is varying in the range of $8.796 \times 10^{-7}\ m^2/Vs$ to $2.453 \times 10^{-6} m^2/Vs$. The charge carrier density N_C is estimated form a relation $N_C = \sigma/e\mu$ is exist between 3.033×10^{20} and 5.124×10^{22}. $eV^{-1}m^{-3}$ both μ and N_C are exhibited in table 4

and variances in both values as a function of the logarithm are plotted in figure 8. It's conceivable to discern that both $\log \mu$ and $\log N_C$ variants behave in the exact opposite way, mobility is maxima at 0.05 where the charge carrier concentration is minimum that is vanadium ion charge concentration is dominated by manganese ions concentration of these charges grows with respect to the addition of MnO_2 content till 0.25 mole fraction of MnO_2 in the glass matrix at which both vanadium and manganese ions concentration attains maximum value but after 0.25 mol, manganese ion charge concentration is dominated by vanadium ions at which mobility is reduced to a bare minimum and this may be due to localization of charges raking place around manganese ions and thus hinting the mixed transition effect at 0.25 mole fraction of MnO_2. Such similar variations for μ and N_C has been identified by M. S. Al-Assiri et al [67].

Table 2. *Polaron hopping parameters of BVM glasses.*

Glass Sample	Mole fraction of MnO_2	W	σ at 508K	W_H	W_P	W_D	ε_p	θ_D
	x	eV	$(\Omega m)^{-1}$	eV	eV	eV		K
BVM1	0.05	0.304	1.192×10^{-4}	0.182	0.363	0.245	35.297	463
BVM2	0.1	0.269	3.231×10^{-4}	0.161	0.321	0.217	49.426	468
BVM3	0.15	0.288	3.828×10^{-4}	0.172	0.344	0.232	55.186	443
BVM4	0.2	0.280	1.411×10^{-3}	0.167	0.334	0.226	65.448	358
BVM5	0.25	0.355	1.701×10^{-3}	0.212	0.424	0.286	66.023	353
BVM6	0.3	0.408	6.680×10^{-4}	0.243	0.487	0.329	54.130	478

Table 3. *Polaron band width and other parameter of BVM glasses.*

Glass Sample	Mole fraction of MnO_2	J_{SPH}	J_o	J_{wh}	$\upsilon_o \times 10^{12}$	$N(E_F)$	γ_P
	x	(eV)	(eV)	(eV)	Hz	$eV^{-1}m^{-3}$	
BVM1	0.05	0.0175	0.045	0.060	4.821	1.220×10^{27}	18.202
BVM2	0.1	0.0171	0.040	0.054	4.874	2.622×10^{27}	15.931
BVM3	0.15	0.0167	0.043	0.057	4.613	4.194×10^{27}	18.040
BVM4	0.2	0.0141	0.042	0.056	3.728	6.597×10^{27}	21.677
BVM5	0.25	0.0148	0.053	0.071	3.676	1.089×10^{28}	27.873
BVM6	0.3	0.0192	0.061	0.081	4.978	7.906×10^{27}	23.629

Table 4. *Mobility and charge carrier concentration of BVM glasses.*

Glass Sample	Mole fraction of MnO_2	μ	N_C
	x	m^2/Vs	$eV^{-1}m^{-3}$
BVM1	0.05	2.453×10^{-6}	3.033×10^{20}
BVM2	0.1	2.507×10^{-6}	8.044×10^{20}
BVM3	0.15	1.300×10^{-6}	1.838×10^{21}
BVM4	0.2	8.796×10^{-7}	1.001×10^{22}
BVM5	0.25	2.072×10^{-7}l	5.124×10^{22}
BVM6	0.3	1.641×10^{-7}	2.541×10^{22}

3.5. Variable Range Hopping Conduction

As the non-linear conductivity range cannot be explained by Mott's Small Polaron Hopping model due to the distinct nature of the process responsible for conduction in the non-linear range, where the system's entropy dominates the polaron binding energy that Mott described in terms of a single phonon prediction. The following Motts relationship can be used to interpret the observed nonlinearities in conductivity measurements below the Debye temperature [6, 46, 49].

$$\sigma = B\, e^{(A/T^{-1/4})}$$

$$\text{Here, } A = 4[2\alpha^3/9\pi k N_{MVRH}]^{\frac{1}{4}}$$

$$B = [e^2/2(8\pi)^{\frac{1}{2}}]\upsilon_0\, [N_{MVRH}/\alpha kT]^{\frac{1}{2}}$$

Here, N_{MVRH} is the density of states at the fermi-level, α is a localised state's wave function decay, and $\upsilon_o = k\theta_D/h$ is the optical phonon frequency calculated form the Debye temperature θ_D, with h and k being Planck's constant, Boltzmann's constant respectively. The slopes of the graph of ln σ Vs $T^{-1/4}$ as shown in figure 9 can be used to determine the values of A and B. The density of states, N_{MVRH}, was derived from figure 9 and calculated values lies between $2.06\times 10^{-28}\, eV^{-1}m^{-3}$ and $1.72 \times 10^{-30}\ eV^{-1}m^{-3}$, as shown in table 5, the order of the values obtained are in close agreement with other such glass systems [53, 68, 69]. It is obvious from the density of states data that, N_{MVRH} rises from 0.05 to 0.15 mole fraction of MnO_2, then decreases and climbs again at 0.25 mole fraction, and then decreases abruptly at 0.3 mole fraction of MnO_2 content. With the exception of 0.15 mole, fluctuation of density of states, N_{MVRH} from 0.05 mole to 0.25 mole percentage of MnO_2 content confirmed a comparable tendency to that of mixed transition effect (MTE) of conductivity even at low temperature regime of non-linear conductivity hinting us that even at low temperature region BVM glasses obeying mixed conduction effect.

Table 5. *Density of states, N extracted from MVRH and GVRH of BVM glasses.*

Glass Sample	MnO_2	$(N)_{MVRH}$	$(N)_{GVRH}$
	x	$eV^{-1}m^{-3}$	$eV^{-1}m^{-3}$
BVM1	0.05	3.89×10^{28}	1.04×10^{36}
BVM2	0.1	2.62×10^{29}	1.08×10^{36}
BVM3	0.15	1.72×10^{30}	1.17×10^{36}
BVM4	0.2	4.65×10^{28}	1.01×10^{36}
BVM5	0.25	2.44×10^{29}	1.34×10^{36}
BVM6	0.3	2.06×10^{28}	7.92×10^{27}

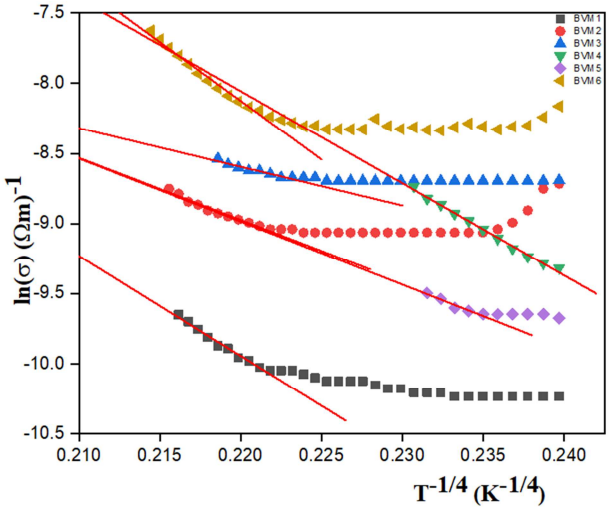

Figure 9. *Plot of* $\ln \sigma$ *Vs* $T^{-1/4}$ *for below Debye temperature data. Solid liens are LS fits to curves of BVM glasses.*

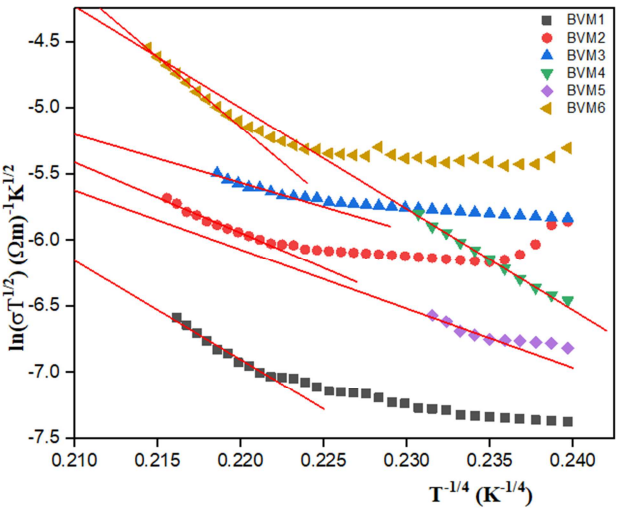

Figure 10. *Plot of* $\ln \sigma T^{1/2}$ *Vs* $T^{-1/4}$ *for below Debye temperature data. Solid liens are LS fits to curves of BVM glasses.*

Variable range hopping (VRH) has been analyzed in the light of Greave's VRH model, which assumes an equivalent low temperature range, and is given by.

$$\sigma T^{1/2} = Ae^{(-B/T^{1/4})}$$

Here A, B are constants and are determined from the least square linear lines fit to data in the plot of ln $\sigma T^{-1/2}$ Vs $T^{-1/4}$ is shown in figure 10.

The density of states N_{GVRH} was measured from the theoretical expression for constant B and given by $B = 2.1\ [\alpha^3/k_B N(E_F)]^{\frac{1}{4}}$

According to the numerous determined values using Greave's VRH model for alkali and TMI doped oxide glasses [10, 11, 39, 67], the $(N)_{GVRH}$ varies from, 10^{27}- 10^{30} $eV^{-1}m^{-3}$, making it evident that the values determined are very much higher and differ from the values comprising oxide glasses. Thus, it is now evident that Mott's VRH model is appropriate for explaining the variable range hopping in glasses in the low temperature zone.

4. Conclusions

Novel semiconducting ternary borate glass system has been synthesized and their non-crystallinity property has been confirmed form X-ray diffraction. The estimated density at room temperature and oxygen packing density exhibited the similar nature of variations, particularly the variation at 0.25 mole fractions of MnO_2 in the glass matrix in both is hinting the mixed transition effect. Measuring the BVM glasses' DC conductivity at temperatures spanning from 303-523 K. The conductivity value kept on increasing with respect to growing content of MnO_2 in glass matrix up to 0.25 mole, there after it went down drastically, with growing MnO_2 content in the glass matrix, such opposite and nonlinear kind of variations has been seen with activation energy and polaron radius. The rise in conductivity value at high temperature region may be due to the increased number of charge carriers available to hopping and decrease in polaron radius and mean spacing between the TMIs decreases the disorder energy of the system but after 0.25 mol of MnO_2 content in the glass matrix increases disorder energy which triggers the localization of charges around manganese ion thereby hindering the hopping process hence the MnO_2 content at 0.25 mole fraction in the glass matrix. The high temperature conductivity region was analyzed in accordance with Mott's small polaron hopping model and from the same numerous physical and hopping parameters were estimated it is observed that with increase of MnO_2 content in glass matrix the polaron hopping energy W_H, polaron binding energy W_P, increased linearly favoring the SPH, but the density ρ, OPD, Debye temperature θ_D, electron-phonon coupling constant γ_P varied exactly similar with respect to the variations in conductivity. The conductivity of BVM glasses at temperature below $\frac{\theta_D}{2}$ was analyzed with available both Mott's and Mott's and Greaves variable range hopping models, and discovered that our BVM glasses are obeying only Mott's variable range hopping. Thus, indicating all of the above parameters are affirms that the anomaly effect in glass science the mixed transition effect can taking place in the present series of glass systems.

Practical Relevance; Our glass systems' base materials were thoughtfully hand-picked with solid-state battery applications in mind, as their abundance and low cost make them an ideal choice for this purpose. Our prepared glasses are excellent semiconducting materials for battery applications, with conductivities in 10^{-5} to 10^{-3} $(\Omega m)^{-1}$ range. Due to its high conductivity, in particular for glass with

composition $x = 0.25$, can be utilized to build electrodes in solid state batteries. Composition glass systems, which have a higher dielectric constant than increased conductivity, are used as dielectric materials [25] in capacitor manufacturing.

References

[1] L. D. Pye, Borate Glasses, Springer US, Springer US, Boston, MA, 2012. https://doi.org/10.1007/978-1-4684-3357-9.

[2] V. P. Singh, N. M. Badiger, J. Kaewkhao, Radiation shielding competence of silicate and borate heavy metal oxide glasses: Comparative study, J Non Cryst Solids. 404 (2014) 167–173. https://doi.org/10.1016/J.JNONCRYSOL.2014.08.003.

[3] M. S. Hasan, U. Werner-Zwanziger, D. Boyd, Composition-structure-properties relationship of strontium borate glasses for medical applications, J Biomed Mater Res A. 103 (2015) 2344–2354. https://doi.org/10.1002/JBM.A.35361.

[4] M. Bengisu, Borate glasses for scientific and industrial applications: a review, Journal of Materials Science 2015 51: 5. 51 (2015) 2199–2242. https://doi.org/10.1007/S10853-015-9537-4.

[5] I. G. Austin, M. Sayer, Hopping conduction at high electric fields in transition metal ion glasses, Journal of Physics C: Solid State Physics. 7 (1974) 905. https://doi.org/10.1088/0022-3719/7/5/013.

[6] I. G. Austin, N. F. Mott, Metallic and nonmetallic behavior in transition metal oxides, Science (1979). 168 (1970) 71–77. https://doi.org/10.1126/SCIENCE.168.3927.71/ASSET/CC75CA72-79A2-4C36-BEAB-49A0C8C07E5B/ASSETS/SCIENCE.168.3927.71.FP.PNG.

[7] I. G. Austin, N. F. Mott, Polarons in crystalline and non-crystalline materials, Https://Doi.Org/10.1080/00018736900101267. 18 (2006) 41–102. https://doi.org/10.1080/00018736900101267.

[8] A. S. Abouhaswa, Y. S. Rammah, G. M. Turky, Characterization of zinc lead-borate glasses doped with Fe^{3+} ions: optical, dielectric, and ac-conductivity investigations, Journal of Materials Science: Materials in Electronics. 31 (2020) 17044–17054. https://doi.org/10.1007/S10854-020-04262-1.

[9] M. P. Kumar, T. Sankarappa, A. M. Awasthi, Thermal and electrical properties of some single and mixed transition-metal ions-doped tellurite glasses, Physica B Condens Matter. 403 (2008) 4088–4095. https://doi.org/10.1016/J.PHYSB.2008.08.012.

[10] J. S. Ashwajeet, T. Sankarappa, R. Ramanna, T. Sujatha, Study of polaron transport mechanisms in two transition metal ions doped borophosphate glasses, Glass Physics and Chemistry 2016 42: 1. 42 (2016) 27–32. https://doi.org/10.1134/S1087659616010028.

[11] G. Rajashekara, J. Sangamesh, B. Arunkumar, N. Nagaraja, M. Prashant Kumar, Anomalous DC electrical conductivity in mixed transition metal ions doped borate glasses, J Non Cryst Solids. 481 (2018) 289–294. https://doi.org/10.1016/J.JNONCRYSOL.2017.10.056.

[12] A. S. Das, M. Roy, D. Biswas, R. Kundu, A. Acharya, D. Roy, S. Bhattacharya, Ac conductivity of transition metal oxide doped glassy nanocomposite systems: temperature and frequency dependency, Mater Res Express. 5 (2018) 095201. https://doi.org/10.1088/2053-1591/AAD43E.

[13] K. SEGA, Y. KURODA, K. SEGA, D. c. conductivity of V_2O_5–MnO–TeO_2 glasses, J Mater Sci. 33 (1998) 1303–1308. https://doi.org/10.1023/A:1004302431797.

[14] D. Biswas, A. S. Das, R. Mondal, A. Banerjee, A. Dutta, S. Kabi, D. Roy, L. S. Singh, Structural properties and electrical conductivity mechanisms of semiconducting quaternary nanocomposites: Effect of two transition metal oxides, Journal of Physics and Chemistry of Solids. 144 (2020) 109505. https://doi.org/10.1016/J.JPCS.2020.109505.

[15] G. El-Damrawi, A. M. Abdelghany, A. K. Hassan, B. Faroun, Conductivity and morphological studies on iron borosilicate glasses, J Non Cryst Solids. 545 (2020) 120233. https://doi.org/10.1016/J.JNONCRYSOL.2020.120233.

[16] L. Murawski, C. H. Chung, J. D. Mackenzie, Electrical properties of semiconducting oxide glasses, J Non Cryst Solids. 32 (1979) 91–104. https://doi.org/10.1016/0022-3093(79)90066-8.

[17] R. Hisam, A. K. Yahya, H. M. Kamari, Z. A. Talib, R. H. Y. Subban, Anomalous dielectric constant and AC conductivity in mixed transition-metal-ion xFe_2O_3–$(20-x)MnO_2$–$80TeO_2$ glass system, Materials Express. 6 (2016) 149–160. https://doi.org/10.1166/MEX.2016.1286.

[18] M. G. Moustafa, Electrical transport properties and conduction mechanisms of semiconducting iron bismuth glasses, Ceram Int. 42 (2016) 17723–17730. https://doi.org/10.1016/J.CERAMINT.2016.08.097.

[19] T. Sankarappa, M. P. Kumar, G. B. Devidas, N. Nagaraja, R. Ramakrishnareddy, AC conductivity and dielectric studies in V_2O_5–TeO_2 and V_2O_5–CoO–TeO_2 glasses, J Mol Struct. 889 (2008) 308–315. https://doi.org/10.1016/J.MOLSTRUC.2008.02.009.

[20] H. HIRASHIMA, K. NISHII, T. YOSHIDA, Electrical Conductivity of TiO_2-V_2O_5-P_2O_5 Glasses, Journal of the American Ceramic Society. 66 (1983) 704–708. https://doi.org/10.1111/J.1151-2916.1983.TB10533.X.

[21] R. Punia, R. S. Kundu, S. Murugavel, N. Kishore, Hopping conduction in bismuth modified zinc vanadate glasses: An applicability of Mott's model, J Appl Phys. 112 (2012) 113716. https://doi.org/10.1063/1.4768898.

[22] A. Gaddam, A. R. Allu, H. R. Fernandes, G. E. Stan, C. C. Negrila, A. P. Jamale, F. O. Méar, L. Montagne, J. M. F. Ferreira, Role of vanadium oxide on the lithium silicate glass structure and properties, Journal of the American Ceramic Society. 104 (2021) 2495–2505. https://doi.org/10.1111/JACE.17671.

[23] S. Das, A. Madheshiya, M. Ghosh, K. K. Dey, S. S. Gautam, J. Singh, R. Mishra, C. Gautam, Structural, optical, and nuclear magnetic resonance studies of V_2O_5-doped lead calcium titanate borosilicate glasses, Journal of Physics and Chemistry of Solids. 126 (2019) 17–26. https://doi.org/10.1016/J.JPCS.2018.10.030.

[24] D. B. Sable, P. P. Khirade, S. D. Birajdar, A. A. Pandit, K. M. Jadhav, Effect of iron oxide (Fe_2O_3) on the structural, optical, electrical, and dielectric properties of SrO–V_2O_5 glasses, Glass Physics and Chemistry 2017 43: 4. 43 (2017) 302–312. https://doi.org/10.1134/S1087659617040149.

[25] J. Khajonrit, A. Montreeuppathum, P. Kidkhunthod, N. Chanlek, Y. Poo-arporn, S. Pinitsoontorn, S. Maensiri, New transparent materials for applications as supercapacitors: Manganese-lithium-borate glasses, J Alloys Compd. 763 (2018) 199–208. https://doi.org/10.1016/J.JALLCOM.2018.05.300.

[26] P. Butnoi, N. Chanlek, Y. Poo-arporn, S. Pinitsoontorn, S. Maensiri, P. Kidkhunthod, Structure-function of novel glasses for possibility as cathode of Li-ion battery: Lithium manganese borate glasses, J Alloys Compd. 809 (2019) 151811. https://doi.org/10.1016/J.JALLCOM.2019.151811.

[27] Z. S. Iro, C. Subramani, S. S. Dash, ELECTROCHEMICAL SCIENCE A Brief Review on Electrode Materials for Supercapacitor, Int. J. Electrochem. Sci. 11 (2016) 10628–10643. https://doi.org/10.20964/2016.12.50.

[28] M. Pal, B. Roy, M. Pal, Structural Characterization of Borate Glasses Containing Zinc and Manganese Oxides, Journal of Modern Physics. 02 (2011) 1062–1066. https://doi.org/10.4236/JMP.2011.29129.

[29] U. Nissar, J. Ahmad, A. M. Rana, S. H. Bukhari, M. T. Jamil, J. A. Khan, R. Shakeel, M. Y. Nadeem, Electrical Characteristics of MnO_2 Doped Bismuth Borate Glass Systems, J Electron Mater. 47 (2018) 1421–1430. https://doi.org/10.1007/S11664-017-5943-5.

[30] V. Vamsi Priya, G. Upender, M. Prasad, FTIR and ESR studies of VO^{2+} and MN^{2+} doped glasses of system $59B_2O_3$-$10As_2O_3$-(30 - X)PbO-xBaO, Glass Physics and Chemistry. 40 (2014) 144–150. https://doi.org/10.1134/S1087659614020230.

[31] B. Tirumala Rao, S. Cole, Physical and spectroscopic studies on manganese doped zinc alumino lithium borate glasses, Mater Today Proc. 5 (2018) 25815–25822. https://doi.org/10.1016/j.matpr.2018.06.574.

[32] V. Babu, M. Vema, S. Boddu, K. Vijaya Babu, V. Madhuri, B. Suresh, Investigations on Spectroscopic Properties of Manganese Ions in Sodium Lead Alumino Borate Glasses, (2020). https://doi.org/10.21203/rs.3.rs-49497/v1.

[33] J. Ashwajeet, T. Sankarappa, … R. R.-G. P. and, undefined 2016, Study of polaron transport mechanisms in two transition metal ions doped borophosphate glasses, Springer. 42 (2016) 27–32. https://doi.org/10.1134/S1087659616010028.

[34] G. P. Singh, P. Kaur, S. Kaur, D. P. Singh, ROLE OF V 2 O 5 IN STRUCTURAL PROPERTIES OF V 2 O 5-MnO 2-PbO-B 2 O 3 GLASSES, Materials Physics and Mechanics. (2011) 58–63.

[35] V. Kundu, R. L. Dhiman, D. Goyal, D. R. Goyal, A. S. Maan, Physical and electrical properties of semiconducting Fe 2 O 3-V 2 O 5-B 2 O 3 glasses, OPTOELECTRONICS AND ADVANCED MATERIALS-RAPID COMMUNICATIONS. 2 (2008) 428–432. https://www.researchgate.net/publication/264976287 (accessed August 25, 2022).

[36] M. R. Ahmed, K. C. Sekhar, S. Ahammed, V. Sathe, Z. A. Alrowaili, M. Amami, I. O. Olarinoye, M. S. Al-Buriahi, B. T. Tonguc, M. Shareefuddin, Synthesis, physical, optical, structural and radiation shielding characterization of borate glasses: A focus on the role of SrO/Al_2O_3 substitution, Ceram Int. 48 (2022) 2124–2137. https://doi.org/10.1016/J.CERAMINT.2021.09.301.

[37] S. Thirumaran, N. Karthikeyan, Structural Elucidation of Some Borate Glass Specimen by Employing Ultrasonic and Spectroscopic Studies, Journal of Ceramics. 2013 (2013). https://doi.org/10.1155/2013/485317.

[38] C. S. Phani Kumar, L. Srinivasa Rao, K. Aruna Prabha, P. Raghavendra Rao, Effect of zirconium oxide nanoparticles on physical, structural and magnetic properties of Bi_2O_3-B_2O_3-MnO_2 glasses, Ceram Int. 46 (2020) 28292–28299. https://doi.org/10.1016/J.CERAMINT.2020.07.332.

[39] M. M. El-Desoky, Characterization and transport properties of V_2O_5–Fe_2O_3–TeO_2 glasses, J Non Cryst Solids. 351 (2005) 3139–3146. https://doi.org/10.1016/J.JNONCRYSOL.2005.08.004.

[40] B. V. Kumar, T. Sankarappa, M. P. Kumar, S. Kumar, Electronic transport properties of mixed transition metal ions doped borophosphate glasses, J Non Cryst Solids. 355 (2009) 229–234. https://doi.org/10.1016/j.jnoncrysol.2008.11.018.

[41] B. Dutta, N. A. Fahmy, I. L. Pegg, Effect of mixed transition-metal ions in glasses. I. The P_2O_5–V_2O_5–Fe_2O_3 system, J Non Cryst Solids. 351 (2005) 1958–1966. https://doi.org/10.1016/J.JNONCRYSOL.2005.05.005.

[42] G. M. Turky, A. M. Fayad, G. T. El-Bassyouni, M. Abdel-Baki, Dielectric and electrical properties of MoO_3-doped borophosphate glass: dielectric spectroscopy investigations, Journal of Materials Science: Materials in Electronics. 32 (2021) 22417–22428. https://doi.org/10.1007/S10854-021-06728-2/FIGURE S/9.

[43] Samdani, G. A. Alharshan, L. Haritha, K. C. Sekhar, Z. A. Alrowaili, I. O. Olarinoye, M. S. Al-Buriahi, Synthesis and characterization of the optical MgO-BaO-B_2O_3-TeO_2-MnO_2 glass system, Optik (Stuttg). 267 (2022) 169679. https://doi.org/10.1016/J.IJLEO.2022.169679.

[44] V. Kundu, R. L. Dhiman, D. Goyal, A. S. Maan, D. R. Goyal, Structural and Physical Properties of Fe_2O_3-B_2O_3-V_2O_5 Glasses, Researchgate. Net. (2008). https://doi.org/10.1155/2008/937054.

[45] B. Dutta, N. A. Fahmy, I. L. Pegg, Effect of mixed transition-metal ions in glasses. Part III: The P_2O_5–V_2O_5–MnO system, J Non Cryst Solids. 352 (2006) 2100–2108. https://doi.org/10.1016/j.jnoncrysol.2006.02.043.

[46] N. Mott, E. Davis, Electronic processes in non-crystalline materials, 2012th ed., OUP Oxford, 2012. https://books.google.com/books?hl=en&lr=&id=Pl1b_yhKH-YC&oi=fnd&pg=PP1&dq=Mott,+N.+F.,+and+E.+A.+Davis.+%22Electronic+processes+in+non-crystalline+materials,+2nd+edn.+Clarendon.%22+Oxford+(1979).&ots=d7xSaBHXWc&sig=Yu9LHeTmzkbjZ11rVTfz1QVuB20 (accessed August 11, 2022).

[47] A. v. Banagar, M. Prashant Kumar, N. Nagaraja, Effect of Mixed Transition Metal Ions in B_2O_3-V_2O_5-MoO_3 Glass System, Journal of Electronic Materials 2020 49: 12. 49 (2020) 7370–7378. https://doi.org/10.1007/S11664-020-08499-8.

[48] E. M. Ahmed, N. A. El-Ghamaz, S. M. Albhbah, Limited frequency domain of the ac conductivity of some As_2O_3. V_2O_5. CuO. Nd_2O_3 glasses, J Non Cryst Solids. 558 (2021) 120659. https://doi.org/10.1016/J.JNONCRYSOL.2021.120659.

[49] N. F. Mott, Conduction in glasses containing transition metal ions, J Non Cryst Solids. 1 (1968) 1–17. https://doi.org/10.1016/0022-3093(68)90002-1.

[50] S. Annamalai, R. P. Bhatta, I. L. Pegg, B. Dutta, Mixed transition-ion effect in the glass system: Fe_2O_3-MnO-TeO_2, J Non Cryst Solids. 358 (2012) 1380–1386. https://doi.org/10.1016/j.jnoncrysol.2012.03.016.

[51] C. CHUNG, M. JD, M. L, ELECTRICAL PROPERTIES OF SEMICONDUCTING OXIDE GLASSES, ELECTRICAL PROPERTIES OF SEMICONDUCTING OXIDE GLASSES. (1979).

[52] H. Doweidar, I. A. Gohar, A. A. Megahed, G. El-Damrawi, Structure-transport relationships in lead borate glasses containing V_2O_5, Solid State Ion. 46 (1991) 275–281. https://doi.org/10.1016/0167-2738(91)90226-2.

[53] A. Ghosh, B. K. Chaudhuri, DC conductivity of V_2O_5-Bi_2O_3 glasses, J Non Cryst Solids. 83 (1986) 151–161. https://doi.org/10.1016/0022-3093(86)90065-7.

[54] J. Appel, Polarons, in: Solid State Physics - Advances in Research and Applications, Academic Press, 1968: pp. 193–391. https://doi.org/10.1016/S0081-1947(08)60741-9.

[55] A. Satpati, G. R. Kandregula, K. Ramanujam, Machine learning enabled high-throughput screening of inorganic solid electrolytes for regulating dendritic growth in lithium metal anodes, New Journal of Chemistry. 46 (2022) 14227–14238. https://doi.org/10.1039/D2NJ01827F.

[56] H. Satou, H. Sakata, DC Hopping conduction in Fe_2O_3–MgO–TeO_2 glasses, Mater Chem Phys. 65 (2000) 186–191. https://doi.org/10.1016/S0254-0584(00)00242-X.

[57] A. K. Bandyopadhyay, J. O. Isard, S. Parke, Polaronic conduction and spectroscopy of borate glasses containing vanadium, J Phys D Appl Phys. 11 (1978) 2559. https://doi.org/10.1088/0022-3727/11/18/015.

[58] I. A. GOHAR, Y. M. MOUSTAFA, A. A. MEGAHED, E. MANSOUR, Electrical properties of semiconducting barium vanadate glasses containing iron oxide, Physics and Chemistry of Glasses. 39 (1998) 56–60. https://www.ingentaconnect.com/content/sgt/pcg/1998/00000039/00000001/3901056 (accessed August 28, 2022).

[59] P. W. Anderson, Absence of Diffusion in Certain Random Lattices, Physical Review. 109 (1958) 1492–1505. https://doi.org/10.1103/PhysRev.109.1492.

[60] E. Abrahams, P. W. Anderson, T. v. Ramakrishnan, Non-ohmic effects of anderson localization, Philosophical Magazine B. 42 (1980) 827–833. https://doi.org/10.1080/01418638008222330.

[61] D. Emin, Lattice relaxation and small-polaron hopping motion in disordered materials, J Non Cryst Solids. 8–10 (1972) 511–515. https://doi.org/10.1016/0022-3093(72)90185-8.

[62] I. G. Austin, N. F. Mott, Polarons in Crystalline and Non-crystalline Materials, Adv Phys. 18 (1969) 41–102. https://doi.org/10.1080/00018736900101267.

[63] G. N. Greaves, Small polaron conduction in V_2O_5-P_2O_5 glasses, J Non Cryst Solids. 11 (1973) 427–446. https://doi.org/10.1016/0022-3093(73)90089-6.

[64] M. Sayer, A. Mansingh, The application of small polaron theory to transition metal oxide glasses, J Non Cryst Solids. 58 (1983) 91–98. https://doi.org/10.1016/0022-3093(83)90105-9.

[65] M. Pal, K. Hirota, Y. Tsujigami, H. Sakata, Structural and electrical properties of MoO_3-TeO_2 glasses, J Phys D Appl Phys. 34 (2001) 459. https://doi.org/10.1088/0022-3727/34/4/303.

[66] T. Holstein, Studies of polaron motion, Ann Phys (N Y). 8 (1959) 343–389. https://doi.org/10.1016/0003-4916(59)90003-X.

[67] M. S. Al-Assiri, S. A. Salem, M. M. El-Desoky, Effect of iron doping on the characterization and transport properties of calcium phosphate glassy semiconductors, Journal of Physics and Chemistry of Solids. 67 (2006) 1873–1881. https://doi.org/10.1016/J.JPCS.2006.04.015.

[68] A. Srivastava, S. Roy, N. Mehta, A. Dahshan, S. D. Sharma, Studies of low-temperature electrical measurements in some multicomponent selenium rich glassy alloys: Role of sliver modifier, J Non Cryst Solids. 575 (2022) 121171. https://doi.org/10.1016/J.JNONCRYSOL.2021.121171.

[69] A. Malge, T. Sankarappa, T. Sujatha, P. Abdul Azeem, G. B. Devidas, S. Kori, Structural and DC conductivity studies of borotellurite glasses doped with ZnO, Li_2O and Dy_2O_3, Mater Today Proc. 26 (2020) 1960–1963. https://doi.org/10.1016/J.MATPR.2020.02.428.